Measurement of the inclusive jet cross section in $p\bar{p}$ collisions at $\sqrt{s} = 1.96\,\mathrm{TeV}$

V.M. Abazov[36], B. Abbott[75], M. Abolins[65], B.S. Acharya[29], M. Adams[51], T. Adams[49], E. Aguilo[6], S.H. Ahn[31], M. Ahsan[59], G.D. Alexeev[36], G. Alkhazov[40], A. Alton[64,a], G. Alverson[63], G.A. Alves[2], M. Anastasoaie[35], L.S. Ancu[35], T. Andeen[53], S. Anderson[45], B. Andrieu[17], M.S. Anzelc[53], Y. Arnoud[14], M. Arov[60], M. Arthaud[18], A. Askew[49], B. Åsman[41], A.C.S. Assis Jesus[3], O. Atramentov[49], C. Autermann[21], C. Avila[8], C. Ay[24], F. Badaud[13], A. Baden[61], L. Bagby[50], B. Baldin[50], D.V. Bandurin[59], P. Banerjee[29], S. Banerjee[29], E. Barberis[63], A.-F. Barfuss[15], P. Bargassa[80], P. Baringer[58], J. Barreto[2], J.F. Bartlett[50], U. Bassler[18], D. Bauer[43], S. Beale[6], A. Bean[58], M. Begalli[3], M. Begel[73], C. Belanger-Champagne[41], L. Bellantoni[50], A. Bellavance[50], J.A. Benitez[65], S.B. Beri[27], G. Bernardi[17], R. Bernhard[23], I. Bertram[42], M. Besançon[18], R. Beuselinck[43], V.A. Bezzubov[39], P.C. Bhat[50], V. Bhatnagar[27], C. Biscarat[20], G. Blazey[52], F. Blekman[43], S. Blessing[49], D. Bloch[19], K. Bloom[67], A. Boehnlein[50], D. Boline[62], T.A. Bolton[59], G. Borissov[42], T. Bose[77], A. Brandt[78], R. Brock[65], G. Brooijmans[70], A. Bross[50], D. Brown[81], N.J. Buchanan[49], D. Buchholz[53], M. Buehler[81], V. Buescher[22], V. Bunichev[38], S. Burdin[42,b], S. Burke[45], T.H. Burnett[82], C.P. Buszello[43], J.M. Butler[62], P. Calfayan[25], S. Calvet[16], J. Cammin[71], W. Carvalho[3], B.C.K. Casey[50], H. Castilla-Valdez[33], S. Chakrabarti[18], D. Chakraborty[52], K. Chan[6], K.M. Chan[55], A. Chandra[48], F. Charles[19,‡], E. Cheu[45], F. Chevallier[14], D.K. Cho[62], S. Choi[32], B. Choudhary[28], L. Christofek[77], T. Christoudias[43], S. Cihangir[50], D. Claes[67], Y. Coadou[6], M. Cooke[80], W.E. Cooper[50], M. Corcoran[80], F. Couderc[18], M.-C. Cousinou[15], S. Crépé-Renaudin[14], D. Cutts[77], M. Ćwiok[30], H. da Motta[2], A. Das[45], G. Davies[43], K. De[78], S.J. de Jong[35], E. De La Cruz-Burelo[64], C. De Oliveira Martins[3], J.D. Degenhardt[64], F. Déliot[18], M. Demarteau[50], R. Demina[71], D. Denisov[50], S.P. Denisov[39], S. Desai[50], H.T. Diehl[50], M. Diesburg[50], A. Dominguez[67], H. Dong[72], L.V. Dudko[38], L. Duflot[16], S.R. Dugad[29], D. Duggan[49], A. Duperrin[15], J. Dyer[65], A. Dyshkant[52], M. Eads[67], D. Edmunds[65], J. Ellison[48], V.D. Elvira[50], Y. Enari[77], S. Eno[61], P. Ermolov[38], H. Evans[54], A. Evdokimov[73], V.N. Evdokimov[39], A.V. Ferapontov[59], T. Ferbel[71], F. Fiedler[24], F. Filthaut[35], W. Fisher[50], H.E. Fisk[50], M. Ford[44], M. Fortner[52], H. Fox[42], S. Fu[50], S. Fuess[50], T. Gadfort[70], C.F. Galea[35], E. Gallas[50], C. Garcia[71], A. Garcia-Bellido[82], V. Gavrilov[37], P. Gay[13], W. Geist[19], D. Gelé[19], C.E. Gerber[51], Y. Gershtein[49], D. Gillberg[6], G. Ginther[71], N. Gollub[41], B. Gómez[8], A. Goussiou[82], P.D. Grannis[72], H. Greenlee[50], Z.D. Greenwood[60], E.M. Gregores[4], G. Grenier[20], Ph. Gris[13], J.-F. Grivaz[16], A. Grohsjean[25], S. Grünendahl[50], M.W. Grünewald[30], F. Guo[72], J. Guo[72], G. Gutierrez[50], P. Gutierrez[75], A. Haas[70], N.J. Hadley[61], P. Haefner[25], S. Hagopian[49], J. Haley[68], I. Hall[65], R.E. Hall[47], L. Han[7], K. Harder[44], A. Harel[71], R. Harrington[63], J.M. Hauptman[57], R. Hauser[65], J. Hays[43], T. Hebbeker[21], D. Hedin[52], J.G. Hegeman[34], J.M. Heinmiller[51], A.P. Heinson[48], U. Heintz[62], C. Hensel[58], K. Herner[72], G. Hesketh[63], M.D. Hildreth[55], R. Hirosky[81], J.D. Hobbs[72], B. Hoeneisen[12], H. Hoeth[26], M. Hohlfeld[22], S.J. Hong[31], S. Hossain[75], P. Houben[34], Y. Hu[72], Z. Hubacek[10], V. Hynek[9], I. Iashvili[69], R. Illingworth[50], A.S. Ito[50], S. Jabeen[62], M. Jaffré[16], S. Jain[75], K. Jakobs[23], C. Jarvis[61], R. Jesik[43], K. Johns[45], C. Johnson[70], M. Johnson[50], A. Jonckheere[50], P. Jonsson[43], A. Juste[50], E. Kajfasz[15], A.M. Kalinin[36], J.M. Kalk[60], S. Kappler[21], D. Karmanov[38], P.A. Kasper[50], I. Katsanos[70], D. Kau[49], R. Kaur[27], V. Kaushik[78], R. Kehoe[79], S. Kermiche[15], N. Khalatyan[50], A. Khanov[76], A. Kharchilava[69], Y.M. Kharzheev[36], D. Khatidze[70], T.J. Kim[31], M.H. Kirby[53], M. Kirsch[21], B. Klima[50], J.M. Kohli[27], J.-P. Konrath[23], V.M. Korablev[39], A.V. Kozelov[39], J. Kraus[65], D. Krop[54], T. Kuhl[24], A. Kumar[69], A. Kupco[11], T. Kurča[20], J. Kvita[9], F. Lacroix[13], D. Lam[55], S. Lammers[70], G. Landsberg[77], P. Lebrun[20], W.M. Lee[50], A. Leflat[38], J. Lellouch[17], J. Leveque[45], J. Li[78], L. Li[48], Q.Z. Li[50], S.M. Lietti[5], J.G.R. Lima[52], D. Lincoln[50], J. Linnemann[65], V.V. Lipaev[39], R. Lipton[50], Y. Liu[7], Z. Liu[6], A. Lobodenko[40], M. Lokajicek[11], P. Love[42], H.J. Lubatti[82], R. Luna[3], A.L. Lyon[50], A.K.A. Maciel[2], D. Mackin[80], R.J. Madaras[46], P. Mättig[26], C. Magass[21], A. Magerkurth[64], P.K. Mal[55], H.B. Malbouisson[3], S. Malik[67], V.L. Malyshev[36], H.S. Mao[50], Y. Maravin[59], B. Martin[14], R. McCarthy[72], A. Melnitchouk[66], L. Mendoza[8], P.G. Mercadante[5], M. Merkin[38], K.W. Merritt[50], A. Meyer[21], J. Meyer[22,d], T. Millet[20], J. Mitrevski[70], J. Molina[3], R.K. Mommsen[44], N.K. Mondal[29], R.W. Moore[6], T. Moulik[58], G.S. Muanza[20], M. Mulders[50], M. Mulhearn[70], O. Mundal[22], L. Mundim[3], E. Nagy[15], M. Naimuddin[50], M. Narain[77], N.A. Naumann[35], H.A. Neal[64], J.P. Negret[8], P. Neustroev[40], H. Nilsen[23], H. Nogima[3], S.F. Novaes[5], T. Nunnemann[25], V. O'Dell[50], D.C. O'Neil[6], G. Obrant[40], C. Ochando[16], D. Onoprienko[59], N. Oshima[50], N. Osman[43], J. Osta[55], R. Otec[10], G.J. Otero y Garzón[50], M. Owen[44], P. Padley[80], M. Pangilinan[77], N. Parashar[56], S.-J. Park[71], S.K. Park[31], J. Parsons[70], R. Partridge[77], N. Parua[54], A. Patwa[73], G. Pawloski[80], B. Penning[23], M. Perfilov[38], K. Peters[44],

Y. Peters[26], P. Pétroff[16], M. Petteni[43], R. Piegaia[1], J. Piper[65], M.-A. Pleier[22], P.L.M. Podesta-Lerma[33,c],
V.M. Podstavkov[50], Y. Pogorelov[55], M.-E. Pol[2], P. Polozov[37], B.G. Pope[65], A.V. Popov[39], C. Potter[6],
W.L. Prado da Silva[3], H.B. Prosper[49], S. Protopopescu[73], J. Qian[64], A. Quadt[22,d], B. Quinn[66], A. Rakitine[42],
M.S. Rangel[2], K. Ranjan[28], P.N. Ratoff[42], P. Renkel[79], S. Reucroft[63], P. Rich[44], J. Rieger[54], M. Rijssenbeek[72],
I. Ripp-Baudot[19], F. Rizatdinova[76], S. Robinson[43], R.F. Rodrigues[3], M. Rominsky[75], C. Royon[18], P. Rubinov[50],
R. Ruchti[55], G. Safronov[37], G. Sajot[14], A. Sánchez-Hernández[33], M.P. Sanders[17], A. Santoro[3], G. Savage[50],
L. Sawyer[60], T. Scanlon[43], D. Schaile[25], R.D. Schamberger[72], Y. Scheglov[40], H. Schellman[53], T. Schliephake[26],
C. Schwanenberger[44], A. Schwartzman[68], R. Schwienhorst[65], J. Sekaric[49], H. Severini[75], E. Shabalina[51],
M. Shamim[59], V. Shary[18], A.A. Shchukin[39], R.K. Shivpuri[28], V. Siccardi[19], V. Simak[10], V. Sirotenko[50], P. Skubic[75],
P. Slattery[71], D. Smirnov[55], G.R. Snow[67], J. Snow[74], S. Snyder[73], S. Söldner-Rembold[44], L. Sonnenschein[17],
A. Sopczak[42], M. Sosebee[78], K. Soustruznik[9], B. Spurlock[78], J. Stark[14], J. Steele[60], V. Stolin[37], D.A. Stoyanova[39],
J. Strandberg[64], S. Strandberg[41], M.A. Strang[69], E. Strauss[72], M. Strauss[75], R. Ströhmer[25], D. Strom[53],
L. Stutte[50], S. Sumowidagdo[49], P. Svoisky[55], A. Sznajder[3], P. Tamburello[45], A. Tanasijczuk[1], W. Taylor[6],
J. Temple[45], B. Tiller[25], F. Tissandier[13], M. Titov[18], V.V. Tokmenin[36], T. Toole[61], I. Torchiani[23], T. Trefzger[24],
D. Tsybychev[72], B. Tuchming[18], C. Tully[68], P.M. Tuts[70], R. Unalan[65], L. Uvarov[40], S. Uvarov[40], S. Uzunyan[52],
B. Vachon[6], P.J. van den Berg[34], R. Van Kooten[54], W.M. van Leeuwen[34], N. Varelas[51], E.W. Varnes[45],
I.A. Vasilyev[39], M. Vaupel[26], P. Verdier[20], L.S. Vertogradov[36], M. Verzocchi[50], F. Villeneuve-Seguier[43], P. Vint[43],
P. Vokac[10], E. Von Toerne[59], M. Voutilainen[68,e], R. Wagner[68], H.D. Wahl[49], L. Wang[61], M.H.L.S. Wang[50],
J. Warchol[55], G. Watts[82], M. Wayne[55], G. Weber[24], M. Weber[50], L. Welty-Rieger[54], A. Wenger[23,f],
N. Wermes[22], M. Wetstein[61], A. White[78], D. Wicke[26], G.W. Wilson[58], S.J. Wimpenny[48], M. Wobisch[60],
D.R. Wood[63], T.R. Wyatt[44], Y. Xie[77], S. Yacoob[53], R. Yamada[50], M. Yan[61], T. Yasuda[50], Y.A. Yatsunenko[36],
K. Yip[73], H.D. Yoo[77], S.W. Youn[53], J. Yu[78], A. Zatserklyaniy[52], C. Zeitnitz[26], T. Zhao[82], B. Zhou[64],
J. Zhu[72], M. Zielinski[71], D. Zieminska[54], A. Zieminski[54,‡], L. Zivkovic[70], V. Zutshi[52], and E.G. Zverev[38]

(The DØ Collaboration)

[1]Universidad de Buenos Aires, Buenos Aires, Argentina
[2]LAFEX, Centro Brasileiro de Pesquisas Físicas, Rio de Janeiro, Brazil
[3]Universidade do Estado do Rio de Janeiro, Rio de Janeiro, Brazil
[4]Universidade Federal do ABC, Santo André, Brazil
[5]Instituto de Física Teórica, Universidade Estadual Paulista, São Paulo, Brazil
[6]University of Alberta, Edmonton, Alberta, Canada,
Simon Fraser University, Burnaby, British Columbia,
Canada, York University, Toronto, Ontario, Canada,
and McGill University, Montreal, Quebec, Canada
[7]University of Science and Technology of China, Hefei, People's Republic of China
[8]Universidad de los Andes, Bogotá, Colombia
[9]Center for Particle Physics, Charles University, Prague, Czech Republic
[10]Czech Technical University, Prague, Czech Republic
[11]Center for Particle Physics, Institute of Physics,
Academy of Sciences of the Czech Republic, Prague, Czech Republic
[12]Universidad San Francisco de Quito, Quito, Ecuador
[13]LPC, Univ Blaise Pascal, CNRS/IN2P3, Clermont, France
[14]LPSC, Université Joseph Fourier Grenoble 1, CNRS/IN2P3,
Institut National Polytechnique de Grenoble, France
[15]CPPM, IN2P3/CNRS, Université de la Méditerranée, Marseille, France
[16]LAL, Univ Paris-Sud, IN2P3/CNRS, Orsay, France
[17]LPNHE, IN2P3/CNRS, Universités Paris VI and VII, Paris, France
[18]DAPNIA/Service de Physique des Particules, CEA, Saclay, France
[19]IPHC, Université Louis Pasteur et Université de Haute Alsace, CNRS/IN2P3, Strasbourg, France
[20]IPNL, Université Lyon 1, CNRS/IN2P3, Villeurbanne, France and Université de Lyon, Lyon, France
[21]III. Physikalisches Institut A, RWTH Aachen, Aachen, Germany
[22]Physikalisches Institut, Universität Bonn, Bonn, Germany
[23]Physikalisches Institut, Universität Freiburg, Freiburg, Germany
[24]Institut für Physik, Universität Mainz, Mainz, Germany
[25]Ludwig-Maximilians-Universität München, München, Germany
[26]Fachbereich Physik, University of Wuppertal, Wuppertal, Germany
[27]Panjab University, Chandigarh, India
[28]Delhi University, Delhi, India

[29] *Tata Institute of Fundamental Research, Mumbai, India*
[30] *University College Dublin, Dublin, Ireland*
[31] *Korea Detector Laboratory, Korea University, Seoul, Korea*
[32] *SungKyunKwan University, Suwon, Korea*
[33] *CINVESTAV, Mexico City, Mexico*
[34] *FOM-Institute NIKHEF and University of Amsterdam/NIKHEF, Amsterdam, The Netherlands*
[35] *Radboud University Nijmegen/NIKHEF, Nijmegen, The Netherlands*
[36] *Joint Institute for Nuclear Research, Dubna, Russia*
[37] *Institute for Theoretical and Experimental Physics, Moscow, Russia*
[38] *Moscow State University, Moscow, Russia*
[39] *Institute for High Energy Physics, Protvino, Russia*
[40] *Petersburg Nuclear Physics Institute, St. Petersburg, Russia*
[41] *Lund University, Lund, Sweden, Royal Institute of Technology and Stockholm University,*
Stockholm, Sweden, and Uppsala University, Uppsala, Sweden
[42] *Lancaster University, Lancaster, United Kingdom*
[43] *Imperial College, London, United Kingdom*
[44] *University of Manchester, Manchester, United Kingdom*
[45] *University of Arizona, Tucson, Arizona 85721, USA*
[46] *Lawrence Berkeley National Laboratory and University of California, Berkeley, California 94720, USA*
[47] *California State University, Fresno, California 93740, USA*
[48] *University of California, Riverside, California 92521, USA*
[49] *Florida State University, Tallahassee, Florida 32306, USA*
[50] *Fermi National Accelerator Laboratory, Batavia, Illinois 60510, USA*
[51] *University of Illinois at Chicago, Chicago, Illinois 60607, USA*
[52] *Northern Illinois University, DeKalb, Illinois 60115, USA*
[53] *Northwestern University, Evanston, Illinois 60208, USA*
[54] *Indiana University, Bloomington, Indiana 47405, USA*
[55] *University of Notre Dame, Notre Dame, Indiana 46556, USA*
[56] *Purdue University Calumet, Hammond, Indiana 46323, USA*
[57] *Iowa State University, Ames, Iowa 50011, USA*
[58] *University of Kansas, Lawrence, Kansas 66045, USA*
[59] *Kansas State University, Manhattan, Kansas 66506, USA*
[60] *Louisiana Tech University, Ruston, Louisiana 71272, USA*
[61] *University of Maryland, College Park, Maryland 20742, USA*
[62] *Boston University, Boston, Massachusetts 02215, USA*
[63] *Northeastern University, Boston, Massachusetts 02115, USA*
[64] *University of Michigan, Ann Arbor, Michigan 48109, USA*
[65] *Michigan State University, East Lansing, Michigan 48824, USA*
[66] *University of Mississippi, University, Mississippi 38677, USA*
[67] *University of Nebraska, Lincoln, Nebraska 68588, USA*
[68] *Princeton University, Princeton, New Jersey 08544, USA*
[69] *State University of New York, Buffalo, New York 14260, USA*
[70] *Columbia University, New York, New York 10027, USA*
[71] *University of Rochester, Rochester, New York 14627, USA*
[72] *State University of New York, Stony Brook, New York 11794, USA*
[73] *Brookhaven National Laboratory, Upton, New York 11973, USA*
[74] *Langston University, Langston, Oklahoma 73050, USA*
[75] *University of Oklahoma, Norman, Oklahoma 73019, USA*
[76] *Oklahoma State University, Stillwater, Oklahoma 74078, USA*
[77] *Brown University, Providence, Rhode Island 02912, USA*
[78] *University of Texas, Arlington, Texas 76019, USA*
[79] *Southern Methodist University, Dallas, Texas 75275, USA*
[80] *Rice University, Houston, Texas 77005, USA*
[81] *University of Virginia, Charlottesville, Virginia 22901, USA and*
[82] *University of Washington, Seattle, Washington 98195, USA*

We report on a measurement of the inclusive jet cross section in $p\bar{p}$ collisions at a center-of-mass energy $\sqrt{s}$ =1.96 TeV using data collected by the D0 experiment at the Fermilab Tevatron Collider corresponding to an integrated luminosity of 0.70 fb^{-1}. The data cover jet transverse momenta from 50 GeV to 600 GeV and jet rapidities in the range -2.4 to 2.4. Detailed studies of correlations between systematic uncertainties in transverse momentum and rapidity are presented, and the cross section measurements are found to be in good agreement with next-to-leading order QCD calculations.

The measurement of the cross section for the inclusive production of jets in hadron collisions provides stringent tests of quantum chromodynamics (QCD). When the transverse momentum (p_T) of the jet with respect to the beam axis is large, contributions from long-distance processes are small and the production of jets can be calculated in perturbative QCD (pQCD). The inclusive jet cross section in $p\bar{p}$ collisions at large p_T is directly sensitive to the strong coupling constant (α_s) and the parton distribution functions (PDFs) of the proton. Deviations from pQCD predictions at large p_T can indicate new physical phenomena not described by the standard model. A measurement over the widest possible rapidity range provides simultaneous sensitivity to the PDFs as well as new phenomena expected to populate mainly low rapidities.

In this Letter, we report on a measurement from the D0 experiment of the inclusive jet cross section in $p\bar{p}$ collisions at a center-of-mass of $\sqrt{s} = 1.96$ TeV. The data sample, collected with the D0 detector during 2004-2005 in Run II of the Fermilab Tevatron Collider, corresponds to an integrated luminosity of $\mathcal{L} = 0.70$ fb^{-1} [1]. The increased $p\bar{p}$ center-of-mass energy between Run I ($\sqrt{s} = 1.8$ TeV) and Run II leads to significant increase in the cross section at large p_T — a factor of three at $p_T \sim 550$ GeV. The cross section is presented in six bins of jet rapidity (y), extending out to $|y| = 2.4$, as a function of jet p_T starting at $p_T = 50$ GeV, and provides the largest data set of the inclusive jet spectra at the Tevatron with the smallest experimental uncertainties to date. The measurement also extends earlier inclusive jet cross section measurements by the CDF and D0 collaborations [2, 3].

The primary tool for jet detection is the finely segmented liquid-argon and uranium calorimeter that has almost complete solid angular coverage [5]. The central calorimeter (CC) covers the pseudorapidity region $|\eta| < 1.1$ and the two endcap calorimeters (EC) extend the coverage up to $|\eta| \sim 4.2$. The intercryostat region (ICR) between the CC and EC contains scintillator-based detectors that supplement the coverage of the calorimeter. The Run II iterative seed-based cone jet algorithm including mid-points [6] with cone radius $\mathcal{R} = \sqrt{(\Delta y)^2 + (\Delta\phi)^2} = 0.7$ in rapidity y and azimuthal angle ϕ is used to cluster energies deposited in calorimeter towers. The same algorithm is used for partons in the pQCD calculations. The binning in jet p_T is commensurate with the measured p_T resolution.

Events are required to satisfy jet trigger requirements. Only jets above a given p_T threshold are kept by the highest level trigger (L3). The luminosity used in this analysis for the different triggers is 0.1, 1.5, 17, 73, 500, and 700 pb^{-1} for the 15, 25, 45, 65, 95, and 125 GeV L3 trigger p_T thresholds, respectively. The jet p_T spectra from different triggers are combined (always with an efficiency > 98%) to form a continuous spectrum in p_T. The

cross section is corrected for jet trigger inefficiencies determined using an independent sample of muon triggered events.

The jet p_T is corrected for the energy response of the calorimeter, energy showering in and out the jet cone, and additional energy from event pile-up and multiple proton interactions. The jet energy corrections fix the calorimeter jet four-momentum to the particle level energy. The electromagnetic part of the calorimeter is calibrated using $Z \to e^+e^-$ events [7]. The jet response for the region $|\eta| < 0.4$ is determined using the momentum imbalance in γ+jet events. The p_T imbalance in dijet events with one jet in $|\eta| < 0.4$ and the other anywhere in η is used to intercalibrate the jet response in η, as a function of jet p_T. Jet energy scale corrections are typically $\sim$50% (20%) of the jet energy at 50 (400) GeV. Further corrections due to the difference in response between quark- and gluon-initiated jets are computed using the PYTHIA [8] event generator, passed through a GEANT-based [9] simulation of the detector response in which the single-pion response was corrected to give the same jet response for data and simulation in γ+jet events. These corrections amount to $\sim +4\%$ at jet energies of 50 GeV and $\sim -2\%$ at 400 GeV in the CC. The relative uncertainty of the jet p_T calibration ranges from 1.2% at $p_T \sim 150$ GeV to 1.5% at 500 GeV in the CC, and 1.5–2% in the ICR and EC .

The position of the $p\bar{p}$ interaction is reconstructed using a tracking system consisting of silicon microstrip detectors and scintillating fibers located inside a solenoidal magnetic field of 2 T [5]. The position of the vertex along the beamline is required to be within 50 cm of the detector center. The signal efficiency of this requirement is 93.0±0.5%. A requirement is placed on the missing transverse energy ($\not{E}_T$) in the event, computed as the transverse component of the vector sum of the momenta in calorimeter cells. The $\not{E}_T$ is required to be < $0.7\,p_T^{\max}$ for $p_T^{\max} < 100$ GeV and < $0.5\,p_T^{\max}$ otherwise, where $p_T^{\max}$ is the maximum uncorrected jet p_T in the event. This requirement suppresses the cosmic ray background and is > 99.5% efficient for signal. Requirements on characteristics of shower development for genuine jets are used to remove the remaining background due to electrons, photons, and detector noise that mimic jets. The efficiency for these requirements is > 99% (> 97.5% in the ICR). After all these requirements, the background is < 0.1% in our sample.

The D0 detector simulation provides a good description of jet properties including characteristics of the shower development. Systematic shifts in $|y|$, 0.01 in the CC, 0.02 in the EC, and 0.04 in the ICR, due primarily to detector and jet algorithm effects are also corrected. The correction to the jet cross section for muons and neutrinos, not reconstructed within jets, is determined using PYTHIA and is 2%, independent of p_T and y.

The corrections for jet migration between bins in p_T

and y due to finite resolution in energy and position are determined in an unfolding procedure, based on the experimental p_T and y resolutions. The jet p_T resolution is obtained using the p_T imbalance in dijet events and is found to decrease from 13% at $p_T \sim 50$ GeV to 7% at $p_T \sim 400$ GeV in both the CC and the EC. The resolution in the ICR is 16% at $p_T \sim 50$ GeV decreasing to 11% at $p_T \sim 400$ GeV. The method to unfold the data uses a four-parameter ansatz function to parametrize the p_T dependence of the jet cross section,

$$ f(p_T) = N \left(\frac{p_T}{\text{GeV}} \right)^{-\alpha} \left(1 - \frac{2 \cosh(y^{\min}) p_T}{\sqrt{s}} \right)^{\beta} e^{-\gamma p_T}. $$

Here $y^{\min}$ is the lowest edge of the $|y|$ bin and the four varied parameters are N, α, β, and γ. This ansatz function is convoluted with the measured p_T resolution and fitted to the experimental data.

The unfolding corrections vary between 20% at a jet $p_T \sim 50$ GeV and 40% at 400 GeV in the CC. In the EC and the ICR, the corrections are less than 20% at $p_T \sim 50$ GeV, but increase to 80% at the largest p_T and y. The fraction of reconstructed jets in one bin after smearing, originating from the same bin, is small ($\sim 20\%$) for the most forward y bin at high p_T due to the p_T resolution. The highest p_T bins at high $|y|$ considered in this analysis are required to have an expected probability for the measurement to arise from p_T resolution effects below 5%. The y resolution is better than 0.05 (0.01) for jets with $p_T \sim 50$ GeV (400 GeV), and leads to a migration correction less than 2% in most bins, and 10% in the highest y bin.

The results of the inclusive jet cross section measurement corrected to particle level are displayed in Fig. 1 in six $|y|$ bins as a function of p_T. The cross section extends over more than eight orders of magnitude from $p_T = 50$ GeV to $p_T > 600$ GeV. Perturbative QCD predictions to next-to-leading order (NLO) in α_S, computed using the FASTNLO program [10] (based on NLOJET++ [11]) and the PDFs from CTEQ6.5M [12], are compared to the data. The renormalization and factorization scales (μ_R and μ_F) are set to the individual jet p_T. The predictions are corrected for non-perturbative contributions due to the underlying event and hadronization computed by PYTHIA with the CTEQ6.5M PDFs, the QW tune [13], and the two-loop formula for α_S. These non-perturbative corrections to theory extend from +10% to +20% at $p_T \sim 50$ GeV between $|y| < 0.4$ and $2.0 < |y| < 2.4$. The corrections are of order +5% for $p_T \sim 100$ GeV, and smaller than +2% above 200 GeV.

The ratio of the data to the theory is shown in Fig. 2. The dashed lines show the uncertainties due to the different PDFs coming from the CTEQ6.5 parametrizations. The predictions from MRST2004 [14] are displayed by the dotted line. In all y regions, the predictions agree well with the data. There is a tendency for the data to
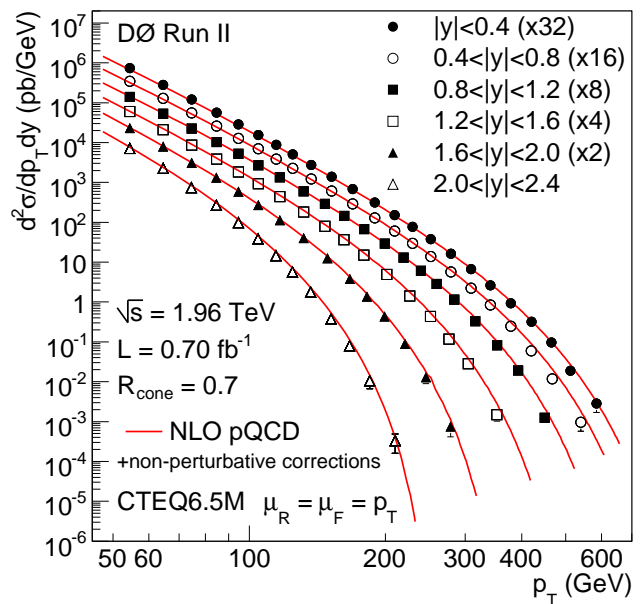

FIG. 1: The inclusive jet cross section as a function of jet p_T in six $|y|$ bins. The data points are multiplied by 2, 4, 8, 16, and 32 for the bins $1.6 < |y| < 2.0$, $1.2 < |y| < 1.6$, $0.8 < |y| < 1.2$, $0.4 < |y| < 0.8$, and $|y| < 0.4$, respectively.

be lower than the central CTEQ prediction — particularly at very large p_T — but mostly within the CTEQ PDF uncertainty band. The p_T dependence of the data is well reproduced by the MRST parametrization. The experimental systematic uncertainty is comparable to the PDF uncertainties. The theoretical scale uncertainty, obtained by varying the factorization and renormalization scales between $\mu_R = \mu_F = p_T/2$ and $\mu_R = \mu_F = 2p_T$ is typically 10–15%. In most bins, the experimental uncertainties are of the same order as the theoretical uncertainties. Tables of the cross sections together with their uncertainties are given in Ref. [15].

Correlations between systematic uncertainties are studied in detail to increase the value of these data in future PDF fits. Point-to-point correlations in p_T and y are provided for the 24 sources of systematic uncertainty. The relative uncertainties in percent on the cross section measurement are shown in Fig. 3 for the five most significant sources of systematic uncertainty in $|y| < 0.4$ and $2.0 < |y| < 2.4$. The luminosity uncertainty of 6.1%, fully correlated in p_T and y, is not displayed in Fig. 3. The other y bins have similar correlations in shape and values between these two extreme bins. The total uncorrelated uncertainty is $< 3\%$ in the CC, and $< 15\%$ in the EC.

The two largest systematic uncertainties are due to the electromagnetic energy scale obtained from $Z \rightarrow e^+ e^-$ events [7], and the photon energy scale in the CC obtained using the difference in the calorimeter response between photons and electrons in the detector simulation. The uncertainty on the photon energy scale is mainly due
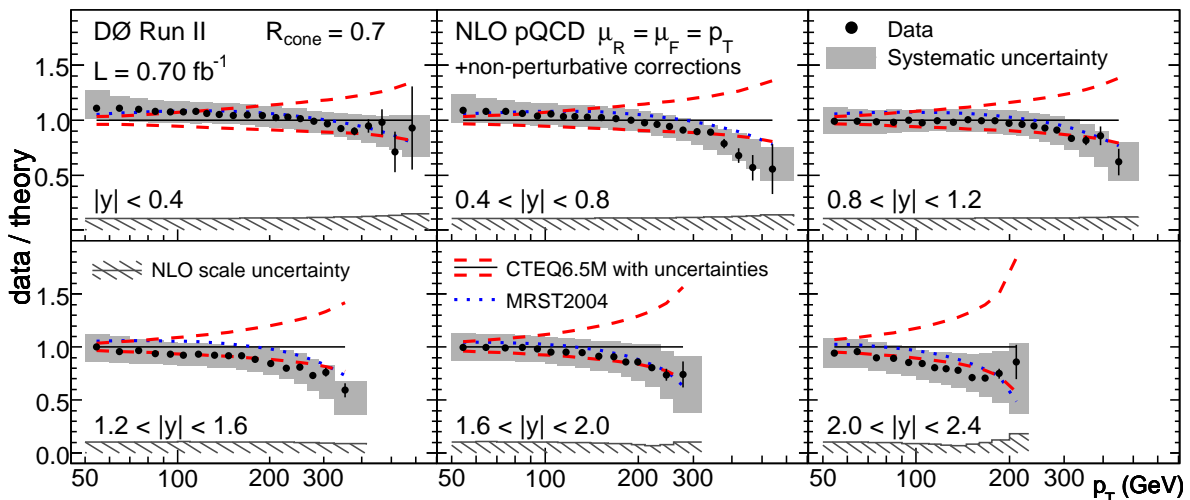
FIG. 2: Measured data divided by theory for the inclusive jet cross section as a function of jet p_T in six $|y|$ bins. The data systematic uncertainties are displayed by the full shaded band. NLO pQCD calculations, with renormalization and factorization scales set to jet p_T using the CTEQ6.5M PDFs and including non-perturbative corrections, are compared to the data. The CTEQ6.5 PDF uncertainties are shown as dashed lines and the predictions with MRST2004 PDFs as dotted lines. The theoretical uncertainty, determined by changing the renormalization and factorization scales between $p_T/2$ and $2p_T$, is shown at the bottom of each figure.

to the limited knowledge of the amount of dead material in front of the calorimeter and from the physics modeling of electromagnetic showers in the GEANT-based [9] simulation. These two contributions to the jet cross section uncertainty are $\sim 5\%$ in the CC and $5-15\%$ in the EC.

The large-p_T extrapolation of jet energy scale is determined using the detector simulation with the single-pion response tuned to γ+jet data. The uncertainty rises to 12% (30%) in the CC (EC), and is dominated by the uncertainty in the jet fragmentation, estimated by comparing the fragmentation models in PYTHIA and HERWIG [16]. The uncertainty in η intercalibration corresponds to systematic uncertainties associated with the procedure to equalize the calorimeter response in different regions of η in dijet events. These systematic uncertainties are negligible in the CC because the η dependent response is calibrated with respect to the CC, but extend up to 25% in the EC. Finally, systematic uncertainties associated with showering effects, due primarily to the modeling of the hadronic shower development in the detector and differences between PYTHIA and HERWIG, range from 3% at low p_T to 7% (15%) at large p_T in the CC (EC).

To show the potential impact of using point-to-point uncertainty correlations in jet p_T and y on PDF determination, we give in Fig. 3 the uncorrelated and total systematic uncertainties as a function of jet p_T as a percentage of the jet cross section measurement. The total uncorrelated uncertainties are less than 15% and 25% of the full uncertainties in the CC and EC respectively. The full systematic uncertainties are similar in size to the PDF uncertainties (Fig. 2) and the detailed analysis

of the correlations which have been performed will make it possible to further constrain the PDFs. Knowledge of these correlations is especially important for constraining the PDFs in NNLO pQCD fits where the uncertainties due to the dependence on the choice of the renormalization and factorization scales are smaller. The point-to-point correlations for the 24 different sources of systematic uncertainties are given in Ref. [15].

In conclusion, the measured inclusive jet cross section corrected for experimental effects to particle level in $p\bar{p}$ collisions at $\sqrt{s} = 1.96$ TeV with $\mathcal{L} = 0.70$ fb^{-1} is presented for six $|y|$ bins as a function of jet p_T, substantially extending the kinematic reach and improving the precision of existing inclusive jet measurements. NLO pQCD calculations with CTEQ6.5M or MRST2004 PDFs agree with the data and favor the lower edge of the CTEQ6.5 PDF uncertainty band at large p_T and the shape of the p_T dependence for MRST2004. A full analysis of correlations between sources of systematic uncertainty is performed, increasing the potential impact of these data in global PDF fits.
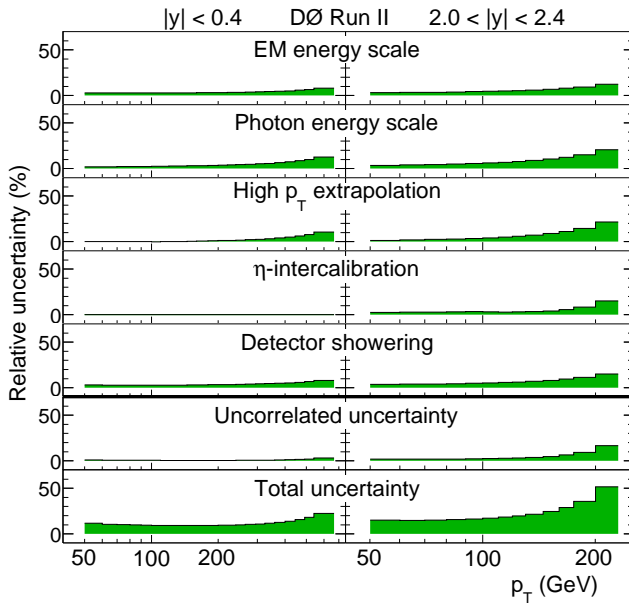
FIG. 3: Correlated uncertainties for $|y| < 0.4$ and $2.0 < |y| < 2.4$ as a function of jet p_T. The five largest systematic uncertainties are shown together with uncorrelated and total uncertainties, computed as the sum in quadrature of all sources.

[a] Visitor from Augustana College, Sioux Falls, SD, USA.
[b] Visitor from The University of Liverpool, Liverpool, UK.
[c] Visitor from ICN-UNAM, Mexico City, Mexico.
[d] Visitor from II. Physikalisches Institut, Georg-August-University, Göttingen, Germany.
[e] Visitor from Helsinki Institute of Physics, Helsinki, Finland.
[f] Visitor from Universität Zürich, Zürich, Switzerland.
[‡] Deceased.

[1] T. Andeen et al., FERMILAB-TM-2365 (2007).
[2] CDF Collaboration, A. Abulencia et al., Phys. Rev. D **75**, 092006 (2007); Phys. Rev. D **74**, 071103 (2006).
[3] D0 Collaboration, B. Abbott et al., Phys. Rev. Lett. **82**, 2451 (1999); Phys. Rev. Lett. **86**, 1707 (2001); CDF Collaboration, F. Abe et al., Phys. Rev. Lett. **77**, 438 (1996).
[4] A. Belyaev et al., JHEP **0601**, 069 (2006).
[5] D0 Collaboration, V.M. Abazov et al., Nucl. Instrum. Methods A **565**, 463 (2006).
[6] G.C. Blazey et al., in Proceedings of the Workshop: "QCD and Weak Boson Physics in Run II", edited by U. Baur, R.K. Ellis, and D. Zeppenfeld, Batavia, Illinois (2000) p. 47.
[7] D0 Collaboration, V.M. Abazov et al., Phys. Rev. D **76**, 012003 (2007).
[8] T. Sjöstrand et al., Comp. Phys. Comm. **135**, 238 (2001).
[9] R. Brun and F. Carminati, CERN Program Library Long Writeup W5013, 1993 (unpublished).
[10] T. Kluge, K. Rabbertz, M. Wobisch, arXiv:hep-ph/0609285.
[11] Z. Nagy, Phys. Rev. D **68**, 094002 (2003).
[12] W.K. Tung et al., JHEP **0702**, 053 (2007); J. Pumplin et al., JHEP **0207**, 12 (2002); D. Stump et al., JHEP **0310**, 046 (2003).
[13] R. Field in: M.G. Albrow et al. [TeV4LHC QCD Working Group], arXiv:hep-ph/0610012.
[14] A.D. Martin et al., Phys. Lett. B **604**, 61 (2004).
[15] Measurements and correlations are available at http://www-d0.fnal.gov /Run2Physics/WWW/results/final/QCD/Q08A/.
[16] G. Marchesini et al., Comp. Phys. Comm. **67**, 465 (1992).